Spatial and Temporal Structure of the Urban Heat Island in Seoul

YEON-HEE KIM

Meteorological Research Institute, Korea Meteorological Administration, Seoul, Korea

JONG-JIN BAIK

School of Earth and Environmental Sciences, Seoul National University, Seoul, Korea

(Manuscript received 18 February 2004, in final form 21 October 2004)

ABSTRACT

The spatial and temporal structure of the urban heat island in Seoul, Korea, is investigated using near-surface temperature data measured at 31 automatic weather stations (AWSs) in the Seoul metropolitan area for the 1-yr period from March 2001 to February 2002. The urban heat island in Seoul deviates considerably from an idealized, concentric heat island structure, mainly because of the location of the main commercial and industrial sectors and the local topography. Relatively warm regions extend in the east–west direction and relatively cold regions are located near the northern and southern mountains. Several warm cores are observed whose intensity, size, and location are found to vary seasonally and diurnally. Similar to previous studies, the urban heat island in Seoul is stronger in the nighttime than in the daytime and decreases with increasing wind speed and cloud cover, but it is least developed in summer. The average maximum urban heat island intensity is 2.2°C over the 1-yr period and it is 3.4°C at 0300 local standard time (LST) and 0.6°C at 1500 LST. The reversed urban heat island is occasionally observed in the afternoon, but its intensity is very weak. An empirical orthogonal function (EOF) analysis is performed to find the dominant modes of variability in the Seoul urban heat island. In the analysis using temperature data that are averaged for each hour of the 1-yr period, the first EOF explains 80.6% of the total variance and is a major diurnal mode. The second EOF, whose horizontal structure is positive in the eastern part of Seoul and is negative in the western part, explains 16.0% of the total variance. This mode is related to the land use type and the diurnal pattern of anthropogenic heat release. In the analysis using temperature data at 0300 LST, the leading four modes explain 72.4% of the total variance. The first EOF reflects that the weakest urban heat island intensity is in summer. It is found that the urban heat island in Seoul is stronger on weekdays than weekends.

1. Introduction

As a result of rapid urbanization and industrialization, numerous environmental problems have emerged, ranging from the local to the global scale. To cope with these problems, we need to monitor and understand environmental changes, especially in urban areas, where most people live and, probably, the largest environmental changes have taken place. On the local and regional scales, much attention has been focused on urban-induced or -modified weather and climate (Changnon 1981; Cotton and Pielke 1995). During the past several decades, extensive studies have been carried out to document the differences in air temperature, wind speed, humidity, precipitation, surface energy flux, boundary layer height, etc., between urban areas and surrounding rural areas, and to explain them (e.g., Olfe and Lee 1971; Garstang et al. 1975; Landsberg 1981; Oke 1982; Lin and Smith 1986; Draxler 1986; Oke 1987; Deosthali 2000; Baik et al. 2001; Shepherd et al. 2002). Among the urban–rural differences, the most notable and well documented is the increase in air temperature in urban areas, called the urban heat island.

Many factors influence urban heat island intensity, including local and synoptic weather, season, time of day, size of the city and its geographical location, urban morphology, and anthropogenic heat. It is well known that the urban heat island intensity is strong on clear and windless nights and exhibits diurnal and seasonal variations (e.g., Yague et al. 1991; Jauregui 1997; Klysik and Fortuniak 1999; Montavez et al. 2000; Morris et al. 2001; Kim and Baik 2002). Oke (1973) and Park (1986) demonstrated that the urban heat island intensity increases as the urban population increases, and they provided functional relations associating urban heat island intensity with population. Kim and Baik (2004) showed

Corresponding author address: Prof. Jong-Jin Baik, School of Earth and Environmental Sciences, Seoul National University, Seoul 151-742, Korea.
E-mail: jjbaik@snu.ac.kr

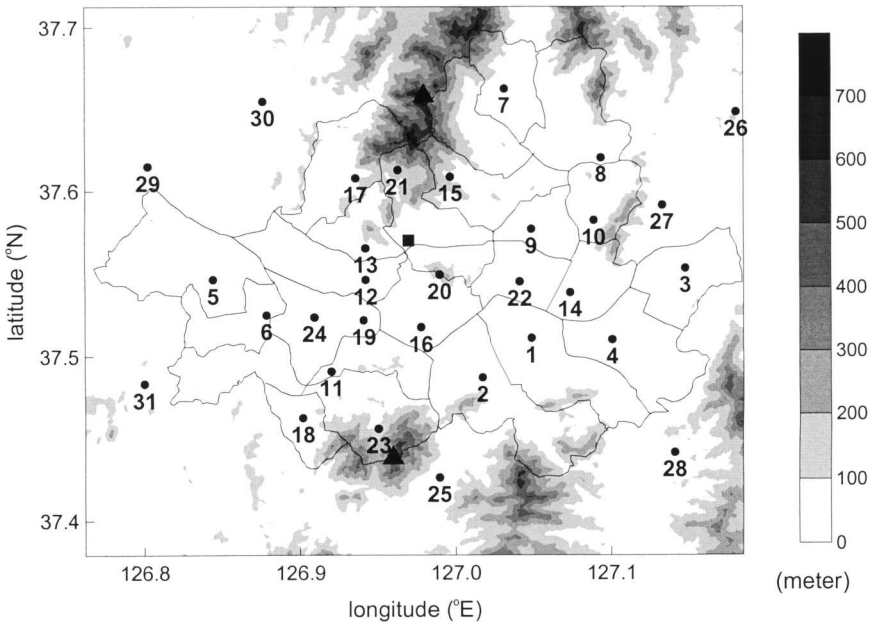

FIG. 1. Location of AWSs in the Seoul metropolitan area. Location of Seoul meteorological observatory is marked as ■. Seoul is divided into 25 administrative subregions, which are demarcated by solid lines. Topography is shaded with linear altitude (above sea level) scales. The peak locations of Mounts Bukhan and Gwanak are marked as ▲.

that the urban heat island intensity in the large cities of Korea tends to be weaker in coastal cities than in inland cities. Ichinose et al. (1999) found that the urban heat island is more intense in winter than in summer because the influence of anthropogenic heat is relatively greater in winter.

At present, the Korea Meteorological Administration (KMA) operates 490 automatic weather stations (AWSs) over the country to provide real-time weather information and also to make better weather forecasts by including AWS data in the KMA data assimilation system. AWSs measure air temperature, wind speed and direction, and precipitation amount. Since its first installment in 1988, the number of AWSs has increased and the quality of AWS data has become more reliable. The density of installed AWSs is high in the Seoul metropolitan area. This provides a good opportunity for studying the spatial and temporal structure of the urban heat island in Seoul. Using AWS data for 4 months of 1999, Boo and Oh (2000) analyzed the urban heat island in Seoul. Their results show that a warm area appears in the central, densely built-up region of the city and that the temperature distribution is related to the land use type and topography.

This study extends Boo and Oh's (2000) earlier work to further characterize the spatial and temporal structure of the urban heat island in Seoul. For this, the near-surface air temperature data, measured at 31 AWSs in the Seoul metropolitan area for a 1-yr period, are analyzed in detail. In particular, an empirical orthogonal function (EOF) analysis is performed to find the dominant modes of variability contained in the original temperature data. Also, the weekday–weekend difference in the Seoul urban heat island is analyzed. In section 2, the data that were used and the EOF analysis method are briefly described. In section 3, the analysis results are presented and discussed. A summary and conclusions are given in section 4.

2. Data and analysis method

Seoul is the capital city of Korea and one of the most densely populated cities in the world. Seoul has a population of about 10 million, about 20% of the total population of Korea. The Han River bisects the city into northern and southern parts. Seoul belongs to the temperate climate zone and has distinct daily and seasonal temperature variations. The annual mean temperature is 12.2°C, the annual mean wind speed is 2.4 m s^{-1}, the annual mean relative humidity is 67%, and the annual precipitation amount is 1344 mm [these are climatological values averaged from 1971 to 2000 (Korea Meteorological Administration 2001)]. In summer, it is hot and humid, receiving much of its annual rainfall in a concentrated period. In winter, Seoul experiences cold and dry weather.

The data used in this study are near-surface air temperatures measured at 31 AWSs in the Seoul metropolitan area for the 1-yr period from March 2001 to February 2002. The data are saved at 1-h intervals. Fig-

ure 1 shows the AWS locations and topography. Seoul is divided into 25 administrative subregions (called gu in Korean), which are demarcated by solid lines in Fig. 1. Twenty-four stations (stations with numbers 1–24 in Fig. 1) are located in Seoul and 7 stations (stations with numbers 25–31 in Fig. 1) are located outside of Seoul. Seoul is, overall, flat. Mount Bukhan, with a highest peak of 837 m, is located in the northern central region, and Mount Gwanak, with a highest peak of 632 m, is located in the southern central region. The fraction of areas covered by mountains in Seoul is, however, small. The Yellow Sea is situated to the west of Seoul. In association with these geographical features, the weather and climate in Seoul are influenced by mountain/valley winds and land/sea breezes, as well as synoptic conditions.

For the 1-yr period from March 2001 to February 2002, in Seoul, the mean temperature is 13.5°C, the mean wind speed is 1.8 m s^{-1}, the mean relative humidity is 61%, and the precipitation amount is 1340 mm. The mean temperature is 1.3°C higher than the climatological mean, but the precipitation amount is similar. Keeping in mind that the urban heat island is influenced by weather conditions, synoptic weather conditions over Korea for each season of the 1-yr period are briefly described here. During the spring, there were many clear and dry days due to the influences of migratory anticyclones approaching the Korean peninsula from the west. Also, a spring drought took place. During summer, there were many hot days at the beginning, and then the heavy rainy period (called Changma in Korean) persisted. After Changma, hot and humid weather followed, with occasional rain showers on local scales. Typhoon Pabuk occurred in August and affected the Korean peninsula. During the autumn, there were many warm and dry days due to the influences of anticyclones that developed in inland China. During winter, there were many cold and dry days due to the influences of cold-air outbreaks associated with Siberian highs.

To investigate the spatial and temporal variability of the urban heat island in Seoul, the EOF analysis, also called the principal component analysis, is carried out. The EOF analysis is a multivariate statistical analysis technique that is widely used in meteorology, which can provide the possibility of reducing a large number of correlated data to a small number of orthogonal functions that explain a large fraction of the total variance. The EOF analysis method splits original data into orthogonal spatial patterns called empirical eigenvectors, and each eigenvector pattern is associated with a series of time coefficients that describes the temporal behavior of a particular spatial mode (Peixoto and Oort 1992). The degree of the contribution of any eigenvector to the total variance is determined by the magnitude of the associated eigenvalue, with the eigenvector associated with the largest eigenvalue accounting for the largest fraction of the total variance in the data (Wilks 1995).

To relate the urban heat island intensity to particular meteorological elements, wind speed and cloudiness data measured at Seoul meteorological observatory (37.57°N, 126.97°E), marked by a symbol ■ in Fig. 1, are utilized. Notice that cloudiness is not measured at AWSs. The observatory data are saved at 3-h intervals. Cloudiness is expressed as values of 0–10, where 0 indicates no clouds and 10 is overcast. When it is rainy or snowy or foggy, cloudiness is assigned the value of 10.

3. Results and discussion

a. Land use classification map

It is well known that the land use type is an important determinant to near-surface air temperature, and a change in land use in an urban location directly influences the temperature therein (Park 1986; Jauregui et al. 1992; Klysik and Fortuniak 1999; Gallo and Owen 1999; Deosthali 2000; Bottyan and Unger 2003). Keeping this in mind, we first present a land use classification map of the Seoul metropolitan area (Fig. 2). This map is constructed using a geographic information system (GIS) for April 1999. The data used for this map are Landsat Thematic Mapper (TM) data with a resolution of 30 m. We expect that the spatial pattern of land use for April 1999 will be very similar to that for April 2001 because no dramatic changes in land use had been made in Seoul during those 2 yr. Main land use types and their fractional areas differ for each gu. Roughly stated, residential and commercial areas are mixed over the city, except for gus having large, green areas. Commercial sectors are densely aggregated in Jung-gu, having station 20, and the southern part of Jongro-gu (the gu north of station 20) and in Gangnam-gu having station 1 (see Figs. 1 and 2). A relatively large number of factories are situated in southwestern Seoul, around the region containing station 18.

b. Structure of the urban heat island

Figure 3 shows the distribution of air temperature averaged for the 1-yr period from March 2001 to February 2002. The spatial pattern of an idealized urban heat island is one in which the temperature decreases outward from a city center, exhibiting nearly concentric isotherms. A typical example of this prototype is documented in Byun (1987). He analyzed aircraft-observed ground surface temperature over the St. Louis, Missouri, metropolitan area on a clear summer afternoon. The urban heat island in Seoul deviates considerably from this prototype, mainly because of the local topography and the location of the main commercial and industrial sectors (i.e., land use type). Figure 3 shows that relatively warm regions extend in the east–west

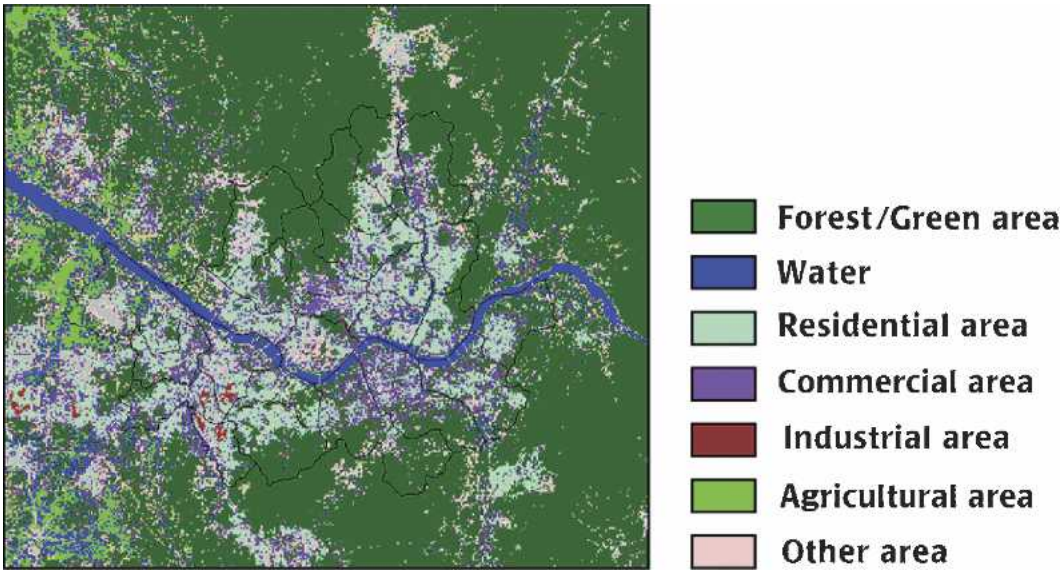

FIG. 2. Land use classification map of the Seoul metropolitan area constructed using GIS. Gu boundaries are demarcated by solid lines. The Han River, bisecting Seoul into northern and southern parts, flows from east to west. This map is for Apr 1999.

direction, and relatively cold regions are located near Mounts Bukhan and Gwanak. Near the borderline of Seoul, the temperature is, as would be expected, relatively low, except near the southwestern and southeastern borderlines, where the sprawling expanse of urbanization is already in progress. Several warm cores are observed. Particularly pronounced are the warm core around station 18 (marked by the letter G), which is surrounded by an industrial complex, and the warm core around station 2 (marked by the letter S), in an area that is highly commercialized, with high-story buildings and heavy traffic. Consistent with previous studies (Park 1986; Jauregui et al. 1992; Klysik and Fortuniak 1999; Gallo and Owen 1999; Deosthali 2000; Bottyan and Unger 2003), Fig. 3 indicates that the distribution of near-surface air temperature within a city is closely linked to the patterns of land use type.

Figure 4 shows the distribution of air temperature averaged for each season in the period from March 2001 to February 2002. The spatial pattern of the seasonal temperature distribution (Fig. 4) is, in general, similar to that of the yearly one (Fig. 3). A temperature distribution exhibiting multiple warm cores is present in each season. In spring, the warm core area in eastern Seoul, including stations 9, 10, 14, and 4, is enlarged in comparison with other seasons. In summer, the warm cores near or south of the Han River appear to merge. In autumn, multiple warm cores reappear. In winter, a warm sector is pronounced in southwestern Seoul, including station 18. As already mentioned, this region is characterized by an industrial complex from which the anthropogenic heat release can be especially large. The effect of anthropogenic heat release on air temperature seems to be relatively large in winter (Ichinose et al. 1999) because the thermal diffusion tends to become smaller in a more stable, cold environment. It is also observed that the temperature gradient in the region including station 18 is largest in winter. Figure 4 documents clearly the seasonal variations of the Seoul urban heat island.

Figure 5 shows the distribution of air temperature averaged for each hour of the 1-yr period. At 0300, 0600, and 0900 local standard time (LST), warm sectors

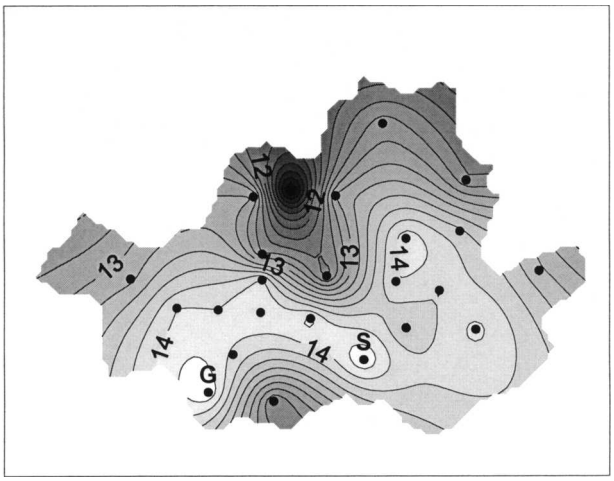

FIG. 3. Distribution of air temperature averaged for the 1-yr period Mar 2001–Feb 2002. The contour interval is 0.2°C. The locations of stations 2 and 18 are marked by letters S and G, respectively.

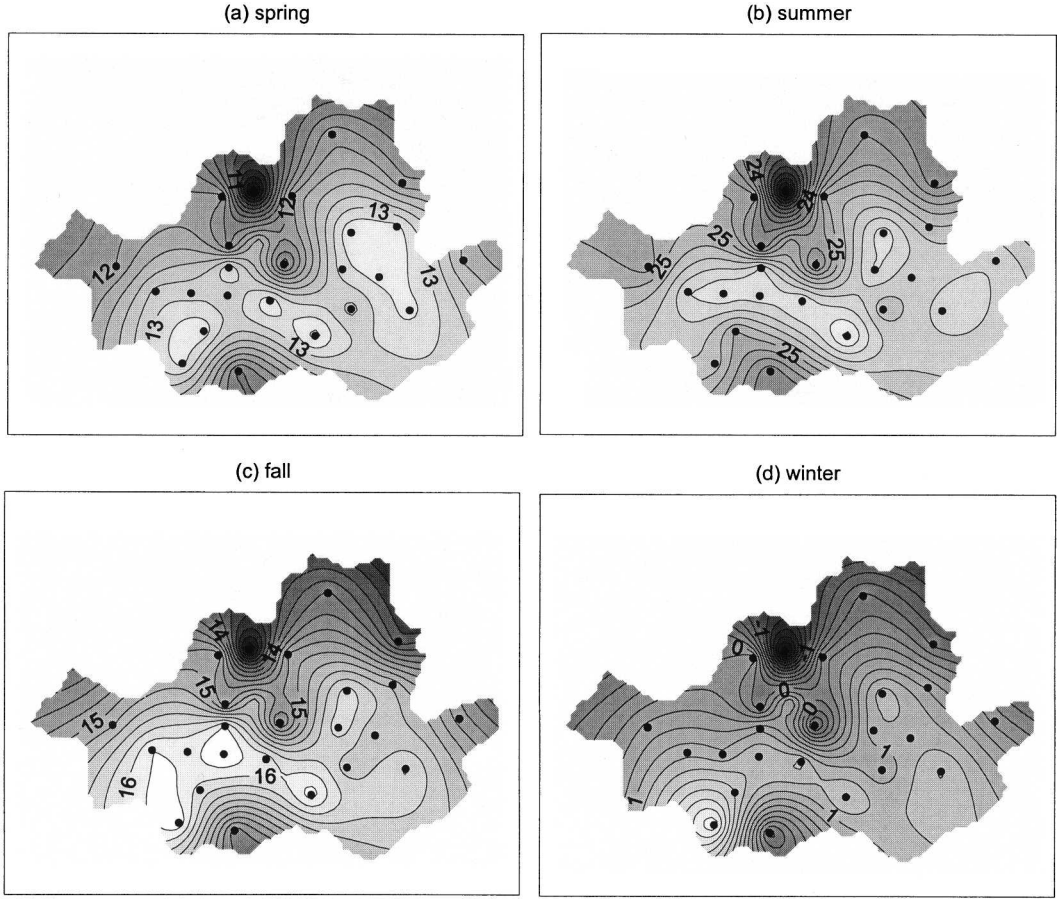

FIG. 4. Distribution of air temperature averaged for each season in the period Mar 2001–Feb 2002. The contour interval is 0.2°C.

stand out in southwestern Seoul. As office hours start, warm sectors appear in some southern and northeastern parts of Seoul, where daytime commercial activity is high. Near close-of-business hours (at 1800 LST), the temperature distribution is fairly homogeneous in the region near or south of the Han River, except for the southern mountain area. At 2100 LST, the warm sector reappears in the industrial and residential area of southwestern Seoul. This diurnal march of the Seoul urban heat island is linked to land use type and the diurnal cycle of human activities.

Using automobile observations from June to August 1982, Park (1986) investigated the characteristics of the Seoul urban heat island. Her study enables us to examine whether there have been any significant changes in the spatial structure of the urban heat island in Seoul during the past two decades. We compare the distribution of temperature anomaly for clear summer nights (2200–2330 LST) in 1982 documented by Park (1986) with the corresponding distribution in 2001 constructed using AWS data (Fig. 6). Here, the temperature anomaly is a temperature deviation from a spatiotemporal mean. Figure 6b is drawn with temperature data at 2200–2400 LST from June to August 2001, under conditions of cloudiness that are less than 5. In both 1982 and 2001, relatively warm regions extend in the east–west direction just south of the Han River. In the temperature anomaly field for 1982, three warm cores with a temperature anomaly larger than 0.4°C appear. Two of them are located just south of the Han River. The other is located in central Seoul, with a maximum temperature anomaly of about 1.2°C. These warm cores correspond to central business and built-up areas. The existence of the negative temperature anomaly region at the corresponding position in central Seoul in 2001 (Fig. 6b) is because station 20 is located on a small mountain, whose station elevation is 262 m. Noticeable changes are observed in southwestern and southeastern Seoul. In 1982, the temperature anomaly in southeastern Seoul and a part of southwestern Seoul is negative. On the other hand, in 2001, the temperature anomaly in southwestern and southeastern Seoul is positive and its magnitude large. These two regions have been rapidly built up during the past 20 yr, thus, exhibiting increases in near-surface air temperature there due to urbanization/industrialization.

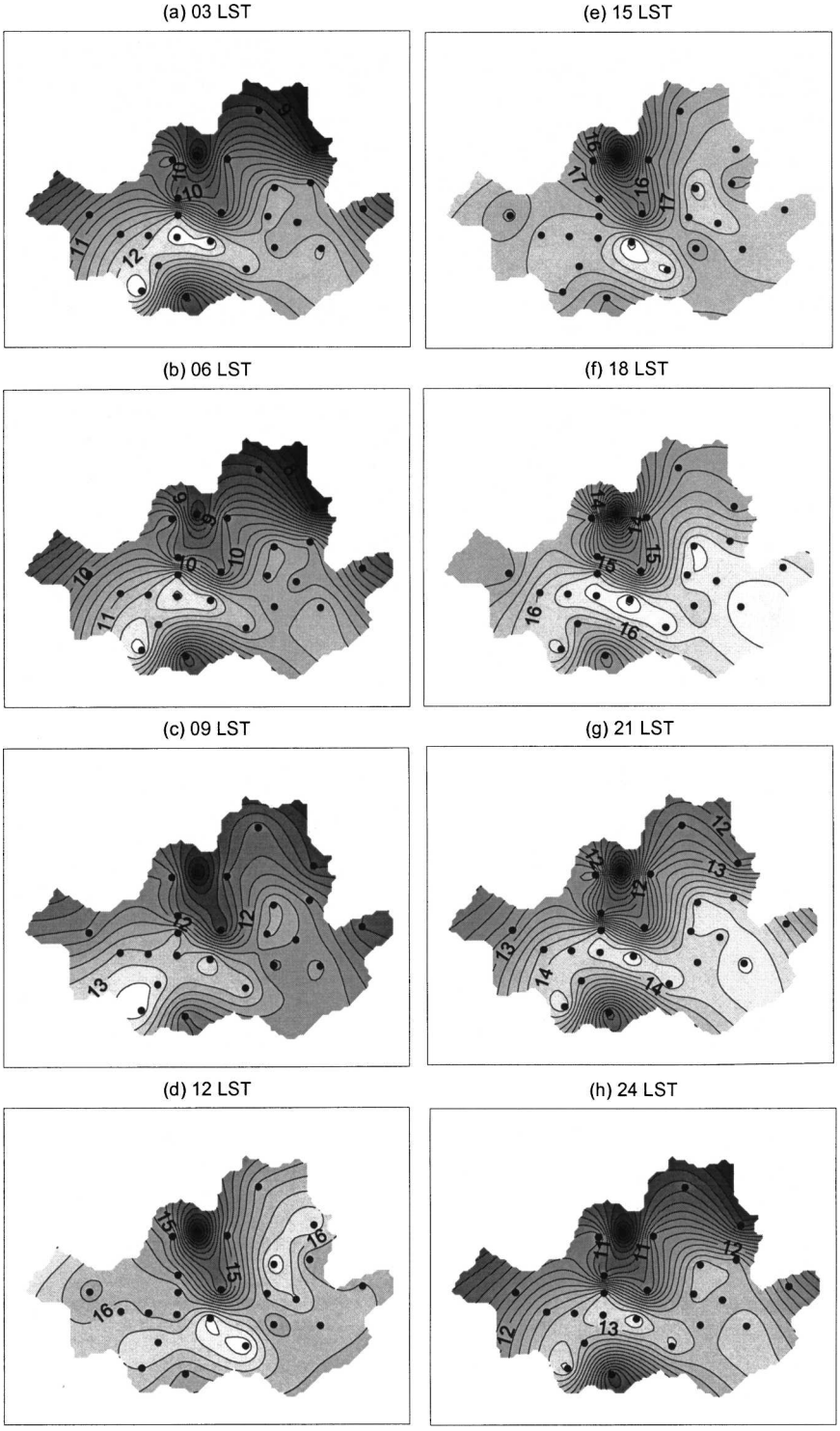

FIG. 5. Distribution of air temperature averaged for each hour of Mar 2001–Feb 2002. The plots are given at 3-h intervals. The contour interval is 0.2°C.

It is noticed that thermometers used by Park (1986)—platinum plated and positioned at about 1.5 m above the ground—have a measurement accuracy up to one decimal point, and those used at the AWSs (PT 100 platinum thermometers) also have the same measurement accuracy. Therefore, the temperature differences found between the two (Figs. 6a and 6b) are significant.

Ichinose et al. (1999) estimated anthropogenic heat

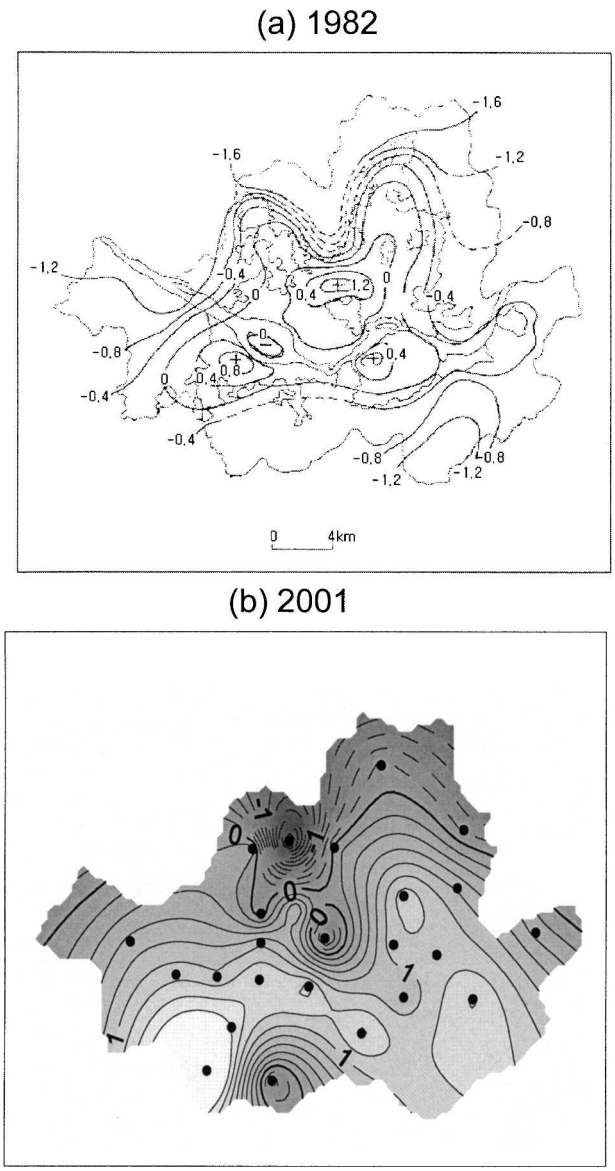

FIG. 6. Distribution of air temperature anomaly for clear summer nights in (a) 1982 [from Park (1986)] and (b) 2001. The contour interval is (a) 0.4° and (b) 0.2°C.

flux in Tokyo, Japan, and their results show its seasonal and diurnal variations. The anthropogenic heat flux in central Tokyo exceeded 400 W m^{-2} in the daytime, and a maximum value was 1590 W m^{-2} in winter. These large values of anthropogenic heat flux and its seasonal and diurnal variations directly affect local air temperature and its seasonal and diurnal variations. We speculate that the pattern of the seasonal and diurnal variations of anthropogenic heat flux and its magnitude in Seoul will not be very different from those in Tokyo because both cities are megalopolises located in Far East Asia, whose energy consumption is probably not very dissimilar. We need to undertake the task of estimating anthropogenic heat flux in Seoul to quantitatively relate the spatial and temporal distributions of anthropogenic heat flux to the urban heat island.

c. Urban heat island intensity

To investigate the temporal characteristics of the urban heat island intensity in Seoul and the influences of meteorological elements on the urban heat island intensity, Seocho (station 2) is selected as an urban site and Sanung (station 26), Nunggok (station 29), and Goyang (station 30) are selected as suburban sites. The air temperature averaged for the 1-yr period from March 2001 to February 2002 is equally the highest at stations 2, 16, and 18 (Fig. 1). Station 16 is very close to the Han River, and station 18 is located in an industrial complex. Therefore, station 2 might be a natural choice for a representative urban site with the highest temperature (see Figs. 1 and 2). There are seven AWSs on the outskirts of Seoul (Fig. 1). Among those, four stations (25, 27, 28, and 31) are situated in already urbanized regions. Therefore, the temperature data at the remaining three suburban stations (Sanung, Nunggok, and Goyang) are utilized to represent suburban temperature. Here, the arithmetic mean of the temperatures at the three stations is taken to obtain the suburban temperature.

The difference between the temperature at Seocho and the three-station-averaged temperature can be approximately regarded as the maximum urban heat island intensity in Seoul, which is plotted in Fig. 7 as the time series at 0300, 0900, 1500, and 2100 LST. The average maximum urban heat island intensity over the 1-yr period is 2.2°C. The urban heat island intensity is stronger in the nighttime (0300 and 2100 LST) than in the daytime (0900 and 1500 LST), exhibiting a diurnal cycle. The average maximum urban heat island intensity is strongest at 0300 LST (3.4°C) and is weakest at 1500 LST (0.6°C). At 0300 LST, the number of days with the urban heat island intensity ≥5°C is 66. At 1500 LST, there are a lot of days in which the urban heat island intensity is negative, that is, the suburban temperature is higher than the urban temperature. This reversed urban heat island is, however, very weak. Figure 7 also indicates that the urban heat island intensity tends to be strong in autumn and weak in summer, exhibiting a seasonal cycle. The seasonal variation of the urban heat island seems to be a characteristic of cities located in monsoonal climates (e.g., Jauregui et al. 1992).

To estimate the urban heat island intensity over the overall city and compare it with the maximum urban heat island intensity (Fig. 7), the urban heat island intensity is calculated as a difference between temperature averaged over Seoul (computed using AWS data at 24 stations within Seoul) and temperature averaged over suburban regions (computed using AWS data at

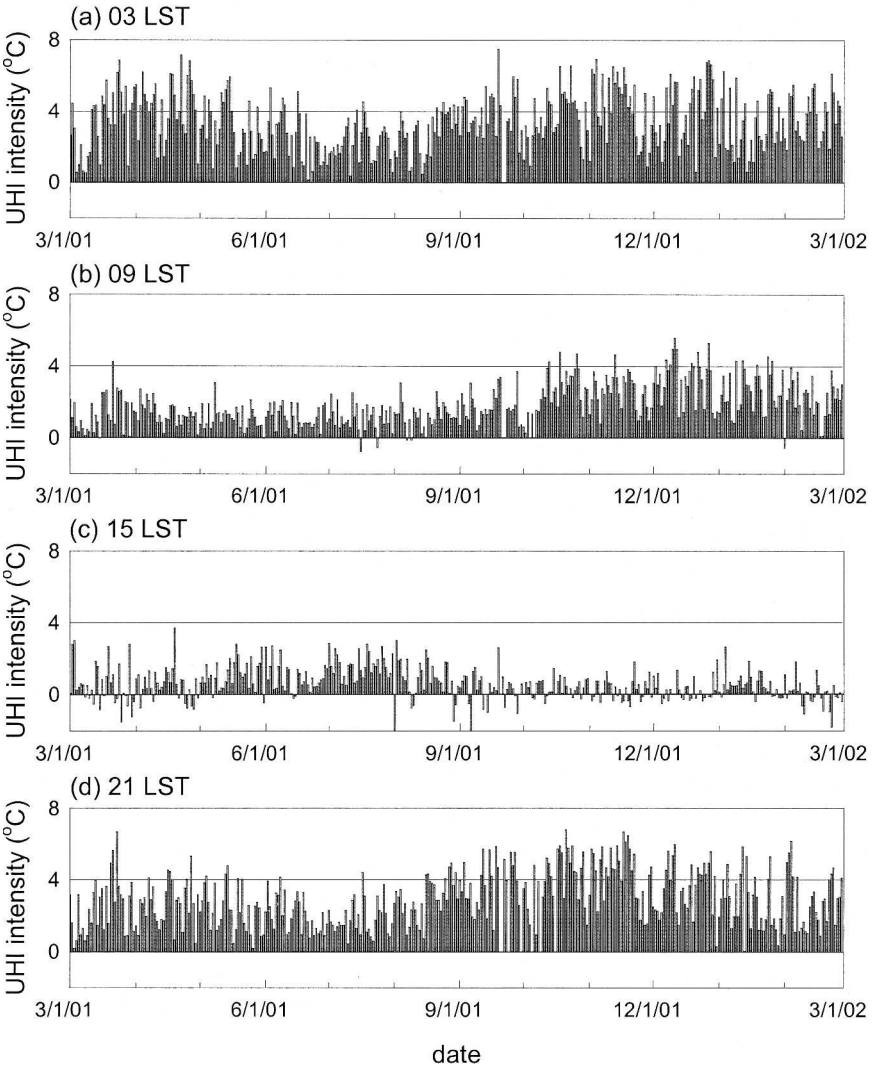

FIG. 7. Time series of difference between air temperature at Seocho and three-station-averaged temperature at (a) 0300, (b) 0900, (c) 1500, and (d) 2100 LST. The names of the three stations are Sanung, Nunggok, and Goyang.

Sanung, Nunggok, and Goyang). At 0300 LST, the average urban heat island intensity over the 1-yr period is 2.5°C, which is 0.9°C weaker than the average maximum urban heat island intensity over the same period (3.4°C).

In Fig. 8, the maximum urban heat island intensity at 0300 LST is related to wind speed and cloudiness. As the wind speed increases, the urban heat island intensity decreases. In comparison with wind speed, the influence of cloudiness on the urban heat island intensity in Seoul is small (as also shown in Kim and Baik 2002).

Figure 9a shows the frequency distribution of daily maximum urban heat island intensity. Here, the daily maximum urban heat island intensity is defined as the daily maximum value of temperature at Seocho minus the three-station-averaged temperature. The frequencies of daily maximum urban heat island intensity (ΔT_{max}) having $0°C \leq \Delta T_{max} < 2°C$, $2°C \leq \Delta T_{max} < 4°C$, $4°C \leq \Delta T_{max} < 6°C$, and $6°C \leq \Delta T_{max} < 8°C$ are 4.7%, 36.7%, 45.2%, and 13.4%, respectively. Figure 9b shows the frequency distribution of the local time of the day when the daily maximum urban heat island intensity is observed. The urban heat island in Seoul is pronounced in the nighttime.

In a recent review article, Arnfield (2003) summarized extensive studies of urban heat islands made during the last 20 yr, which confirm empirical generalizations offered by Oke (1982). These include the following: 1) The urban heat island decreases with increasing wind speed. 2) The urban heat island decreases with increasing cloud cover. 3) The urban heat island inten-

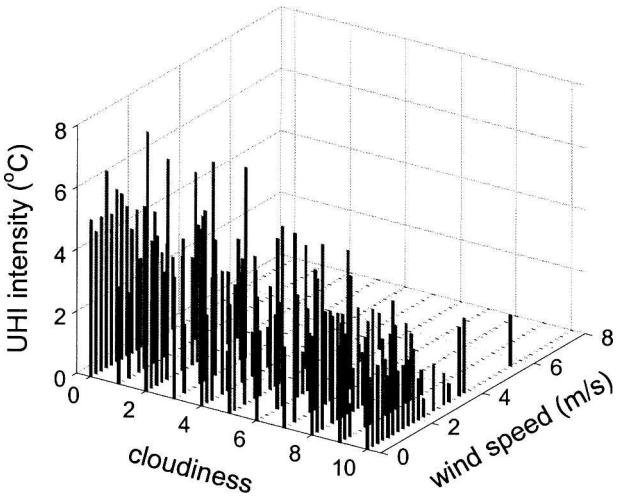

FIG. 8. Urban heat island intensity (difference between air temperature at Seocho and three-station-averaged temperature) in relation to cloudiness and wind speed at 0300 LST. The names of the three stations are Sanung, Nunggok, and Goyang. The unit in the cloudiness axis is tenths of sky covered by clouds.

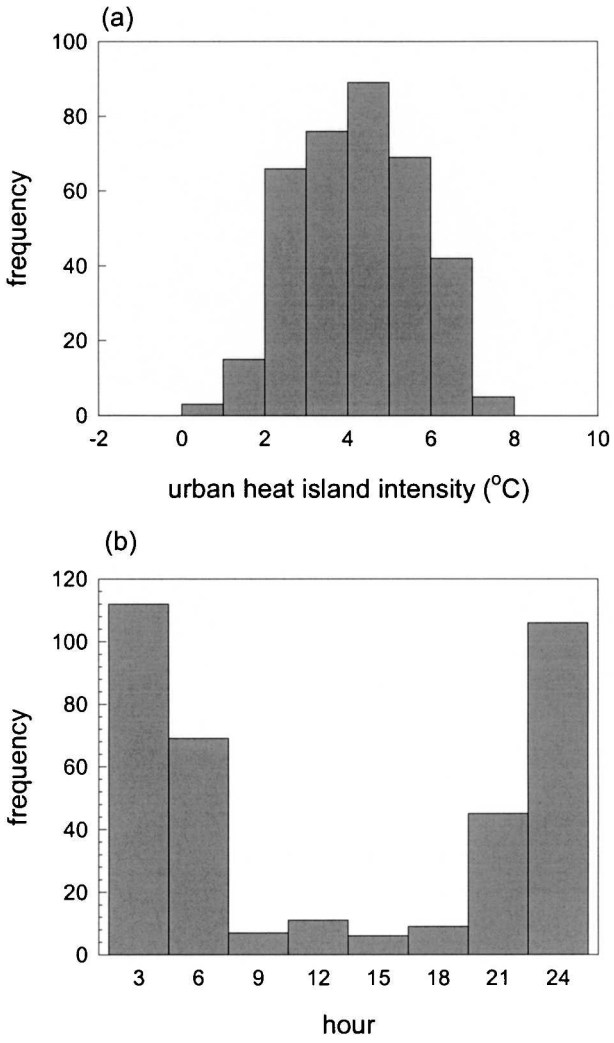

FIG. 9. Frequency distribution of (a) daily maximum urban heat island intensity and (b) local time of its occurrence. The daily maximum urban heat island intensity is defined as the daily maximum value of temperature at Seocho minus averaged temperature at the three stations (Sanung, Nunggok, and Goyang). Here, the frequency is the number of days.

sity is most well developed in summer or in the warm half of the year. 4) The urban heat island intensity is greatest at night. 5) The urban heat island may disappear by day or the city may be cooler than the rural environs.

All of the above generalizations are found in Seoul, except for 3. In Seoul, the urban heat island is least developed in summer. In Korea, days with precipitation and high cloudiness are much more frequent in summer than in other seasons because of the influences of the Asian summer monsoon and the locally developed cloud and precipitation system. For example, in Seoul, the climatological values of annual precipitation amount and the number of annual precipitation days (precipitation day is a day with precipitation amount exceeding 0.1 mm) are 1344 mm and 108, respectively (Korea Meteorological Administration 2001). The precipitation amount in summer (winter) consists of 59% (7%) of the annual precipitation amount. The number of precipitation days in summer (winter) consists of 37% (19%) of the number of annual precipitation days. Much more frequent and intense precipitation events in summer reduce the horizontal contrast in temperature, resulting in the weakest urban heat island in summer. In general, the atmospheric stability in the boundary layer is weaker in summer than in cold seasons, leading to a greater thermal mixing and, thus, less horizontal contrast in temperature. This can also contribute, to some extent, to the least development of the urban heat island in Seoul in summer.

A textbook definition of the urban heat island is, although ambiguous, the difference in near-surface air temperature between urban and surrounding rural/suburban areas. In the traditional two-station approach for urban heat island analysis, an urban station and a rural/suburban station are selected. This approach is adopted in the case that there are a few or only two meteorological stations. In the case that there is an urban station and many stations surrounding a city, a better definition of the urban heat island might be the difference between near-surface air temperature at the urban station and that averaged for representative rural/suburban stations. In the case that there are many stations within a city as well as many rural/suburban stations surrounding it (this study is the case), it is necessary to carefully select a representative urban station(s) for urban heat island analysis because there can be appreciable temperature variations within the city.

In section 3c, Seocho is selected for a representative urban station because this location exhibits the warmest averaged temperature within Seoul, and its nearby region has typical urban characteristics. Therefore, it should be kept in mind that urban heat island intensities for a city can be different according to the urban heat island definitions that are employed. Also, this fact should be in mind when a comparison of urban heat island intensities for different cities is made.

d. EOF analysis

For an EOF analysis, the station-averaged temperature in Seoul is subtracted from air temperature at each station. Figures 10 and 11 show the temporal behavior and spatial display of the first and second EOFs, respectively, that are calculated using air temperatures averaged for each hour from March 2001 to February 2002. The first EOF explains 80.6% of the total variance. The temporal coefficient of the first EOF (Fig. 10) is positive from ~0900 to ~1900 LST and negative from ~2000 to ~0900 LST. That is, it can be said that the temporal coefficient is positive in the daytime and negative in the nighttime. The spatial structure of the first EOF (Fig. 11a) exhibits negative values over a broad area of Seoul, including central, northern central (near Mount Bukhan), southwestern, and southeastern Seoul, and positive values in northeastern, southern central (near Mount Gwanak), westernmost, and easternmost Seoul. Notice that the sprawling expanse of urbanization near and beyond the southwestern and southeastern borderlines is already in progress. Therefore, over a broad area of Seoul, the air temperature anomaly is positive from ~2000 to ~0900 LST and is negative at other times of the day. Recalling that the urban heat island in Seoul is strong in the nighttime and is weak in the daytime, the first EOF is a major diurnal mode in the Seoul urban heat island.

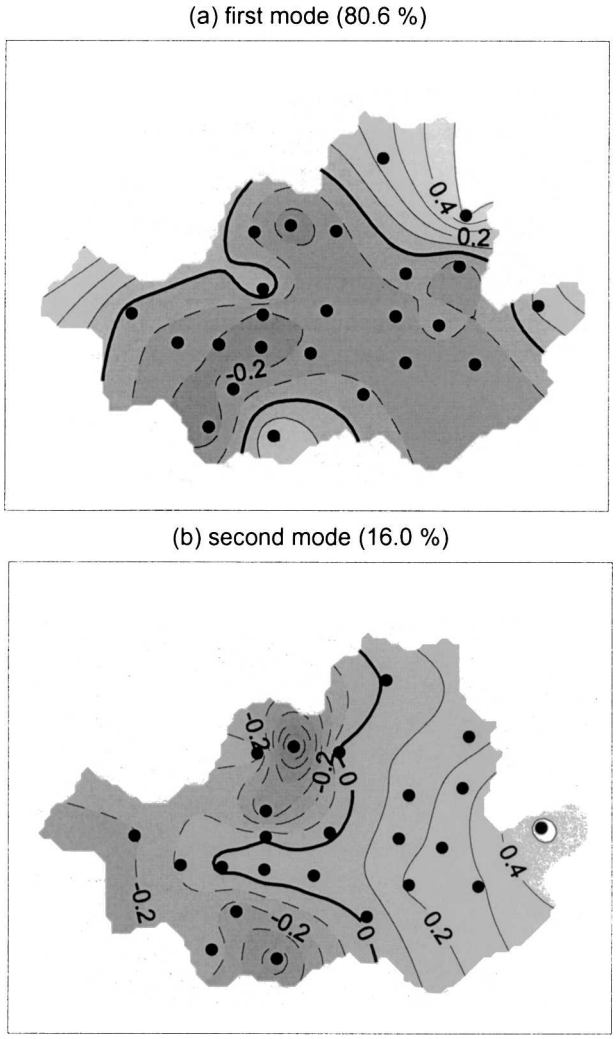

FIG. 11. Spatial display of the first and second EOFs calculated using air temperatures averaged for each hour of Mar 2001–Feb 2002. The contour interval is 0.1.

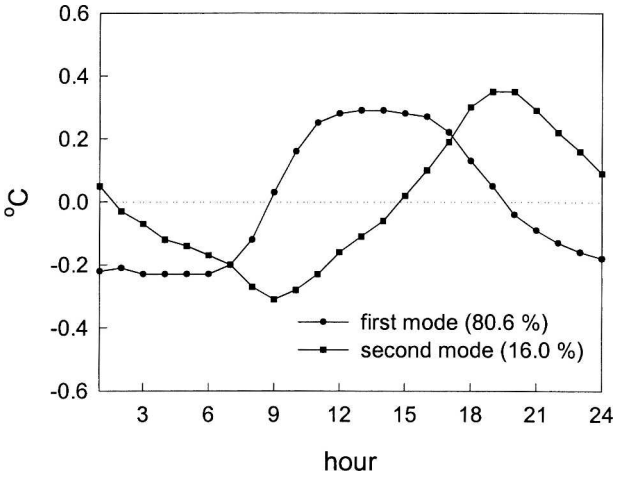

FIG. 10. Temporal behavior of the first and second EOFs calculated using air temperatures averaged for each hour of Mar 2001–Feb 2002.

The second EOF explains 16.0% of the total variance. The temporal coefficient of the second EOF is negative from ~0200 to ~1400 LST and is positive at other times of the day. A minimum temporal coefficient of −0.31°C is observed at 0900 LST (near the beginning of office hours), and a maximum temporal coefficient of 0.35°C is observed at 1900 and 2000 LST (near the end of office hours). A dominant feature in the spatial structure of the second EOF (Fig. 11b) is that the structure is positive in the eastern part of Seoul and is negative in the western part. It is noticeable that a positive region, including stations 16, 19, and 24, intrudes into the negative western part. Therefore, in the eastern part of Seoul, the air temperature anomaly is negative from ~0200 to ~1400 LST and is positive at other times of the day. On the other hand, in the west-

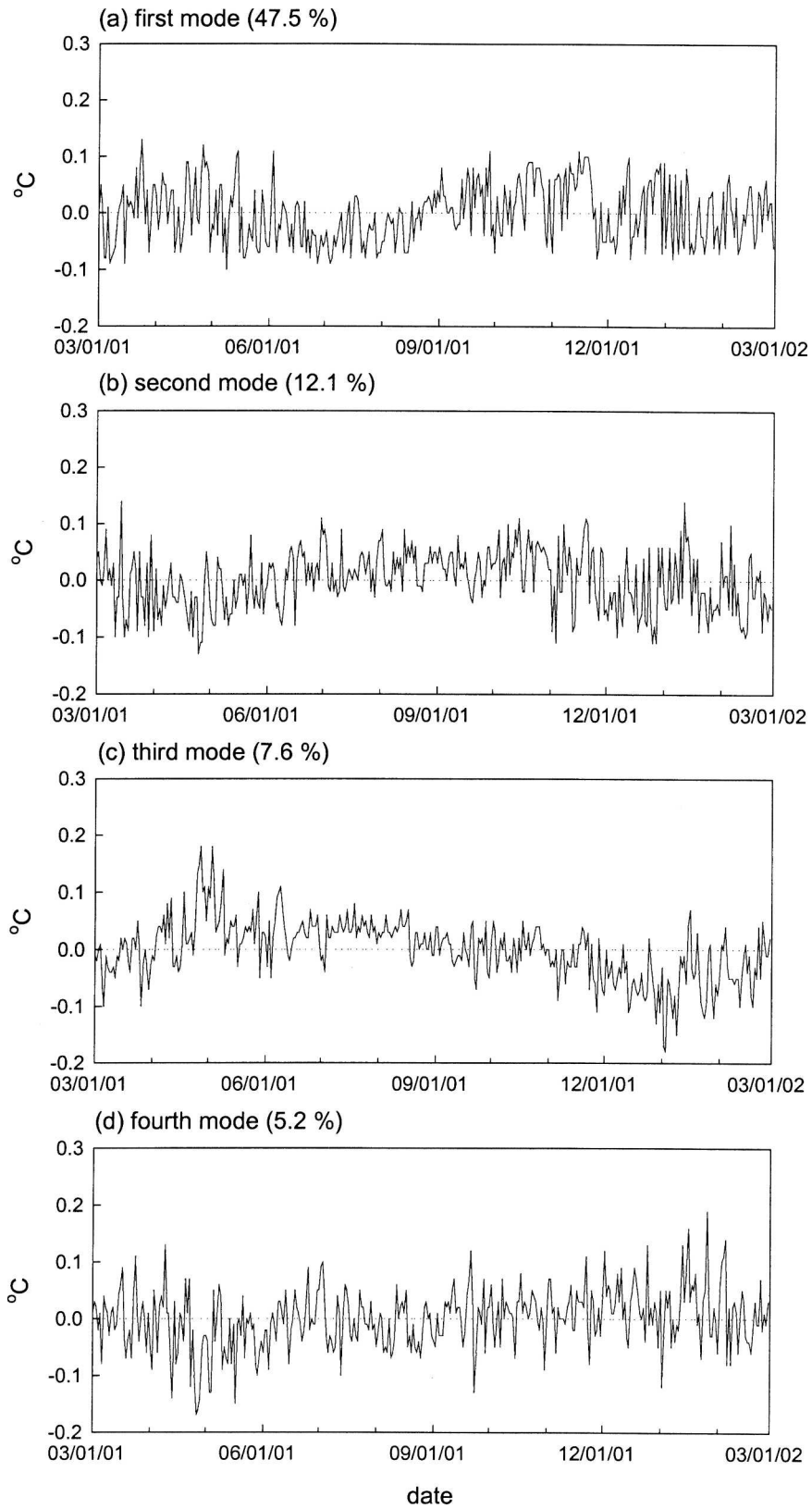

FIG. 12. Temporal behavior of the first, second, third, and fourth EOFs calculated using air temperatures at 0300 LST for Mar 2001–Feb 2002.

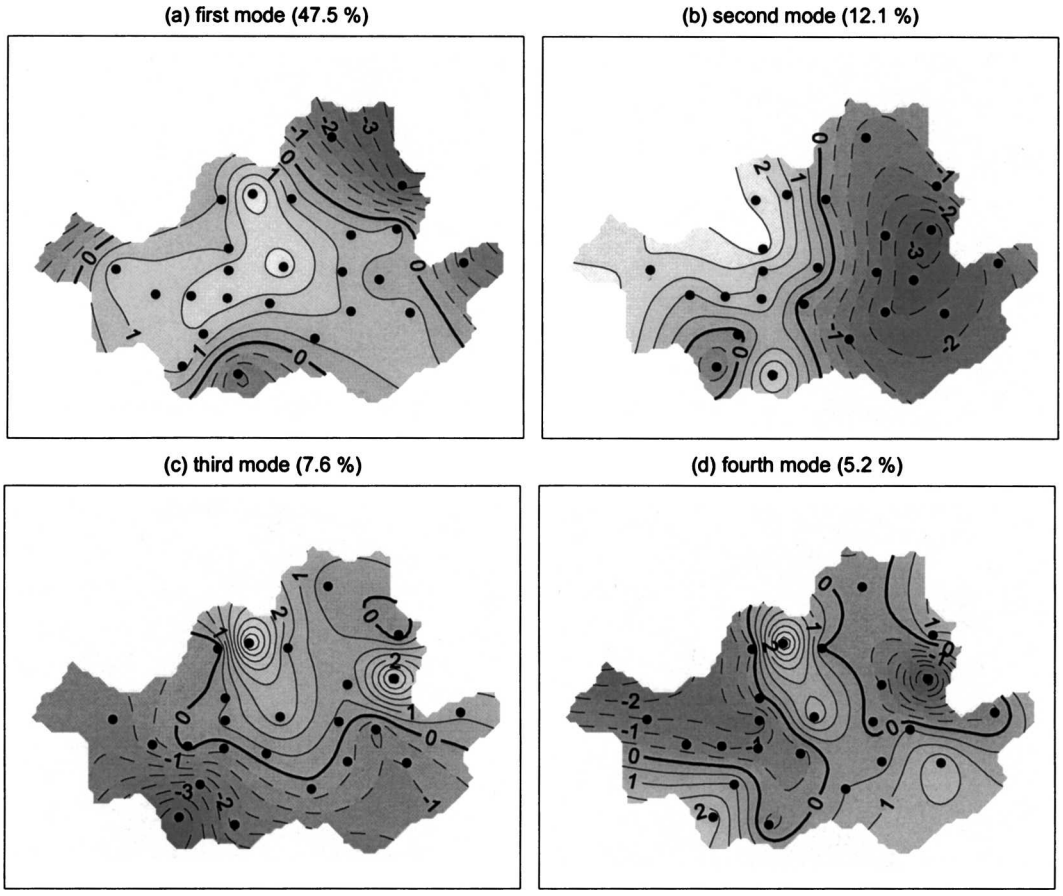

FIG. 13. Spatial display of the first, second, third, and fourth EOFs calculated using air temperatures at 0300 LST for Mar 2001–Feb 2002. The contour interval is 0.5.

ern part of Seoul, the air temperature anomaly is positive from ~0200 to ~1400 LST and is negative at other times. In Seoul, commercial areas are more concentrated in the eastern part than in the western part (see Fig. 2). Anthropogenic heat release from commercial areas has a diurnal cycle, starting at ~0900 LST and ending at ~1900 LST. Hence, the cumulative heat is maximal at ~1900 LST, and its effect is most diminished at ~0900 LST. In this aspect, the second EOF may be called an anthropogenic heat–related diurnal mode of the Seoul urban heat island. The total variance explained by the two leading EOFs is 96.6%.

Figures 12 and 13 show the temporal behavior and spatial display of the four leading EOFs, respectively, calculated using air temperatures at 0300 LST for the 1-yr period. This is the time of day at which the urban heat island in Seoul is pronounced. The first EOF explains about one-half of the total variance (47.5%). The time coefficient of the first EOF (Fig. 12a) tends to be negative with small-amplitude fluctuations in summer as compared with other seasons, reflecting the fact that the urban heat island intensity in Seoul is weakest in summer. The time series of the first EOF (Fig. 12a) is approximately in phase with that of the urban heat island intensity at 0300 LST (Fig. 7a). The spatial structure of the first EOF at 0300 LST (Fig. 13a) is similar to that of the first EOF shown in Fig. 11a, except that the signs are reversed. The first EOF at 0300 LST is a typical mode of the nighttime urban heat island in Seoul.

The second EOF explains 12.1% of the total variance. The spatial structure of the second EOF (Fig. 13b) is positive in the western part of Seoul and is negative in the eastern part, resembling that of the second EOF shown in Fig. 11b, but with opposite signs. The third EOF explains 7.6% of the total variance. The time coefficient of the third EOF (Fig. 12c) tends to be positive in summer and negative in cold months (November–March). The spatial structure of the third EOF (Fig. 13c) is positive in the northern part of Seoul and is negative in the southern and western parts. Thus, in the third EOF, the urban heat island intensity in cold seasons is stronger in the southern and western parts than in the northern part. The

fourth EOF explains 5.2% of the total variance. The total variance explained by the four leading EOFs is 72.4%.

e. Weekday–weekend difference in the urban heat island

Human activities are undertaken on a weekly cycle. Accordingly, it would be interesting to examine whether there is an appreciable difference in the Seoul urban heat island intensity between weekdays and weekends. For this, the data of air temperatures for the 1-yr period from March 2001 to February 2002 are partitioned into weekday and weekend data and then averaged. Figure 14 shows the distribution of weekday temperature, weekend temperature, and their difference (weekday minus weekend). National holidays are treated in the weekend category. In past years, including 2001 and 2002, Saturday was a half-working day (people worked only in the morning) or a nonworking day, depending on employers. Here, Saturdays are treated in the weekend category because a physically more reasonable spatial pattern in the weekday–weekend temperature difference is found when Saturdays are treated in the weekend category than when Saturdays are treated in the weekday category. Figure 14 does show that the weekday temperature is higher than the weekend temperature, that is, the urban heat island in Seoul is stronger on weekdays than weekends. Three regions with lighter or no shading in southern Seoul (regions around stations 6, 19, and 1, from the left in Fig. 14c) exhibit appreciable weekday–weekend temperature differences. These regions are characterized by heavy traffic or high commercial activities on weekdays. The temperature differences at stations 6, 19, and 1 are 0.55°, 0.60°, and 0.49°C, respectively. In coming years, Saturday will be fully a nonworking day. Then, the weekday–weekend temperature difference is expected to be larger than that shown in Fig. 14c.

4. Summary and conclusions

Using near-surface air temperature data measured at 31 automatic weather stations (AWSs) for the 1-yr period from March 2001 to February 2002, the spatial and temporal structure of the urban heat island in Seoul was examined in detail. It was found that the Seoul urban heat island deviates considerably from an idealized, concentric heat island pattern. This can be mainly attributed to the location of the main commercial and industrial sectors and the local topography. Several warm cores were observed, and their intensity, size, and location were shown to vary seasonally and diurnally. It was found that the urban heat island in Seoul is stronger in the nighttime than in the daytime, and decreases with increasing wind speed and cloud cover, but it is least developed in summer. The reversed urban heat

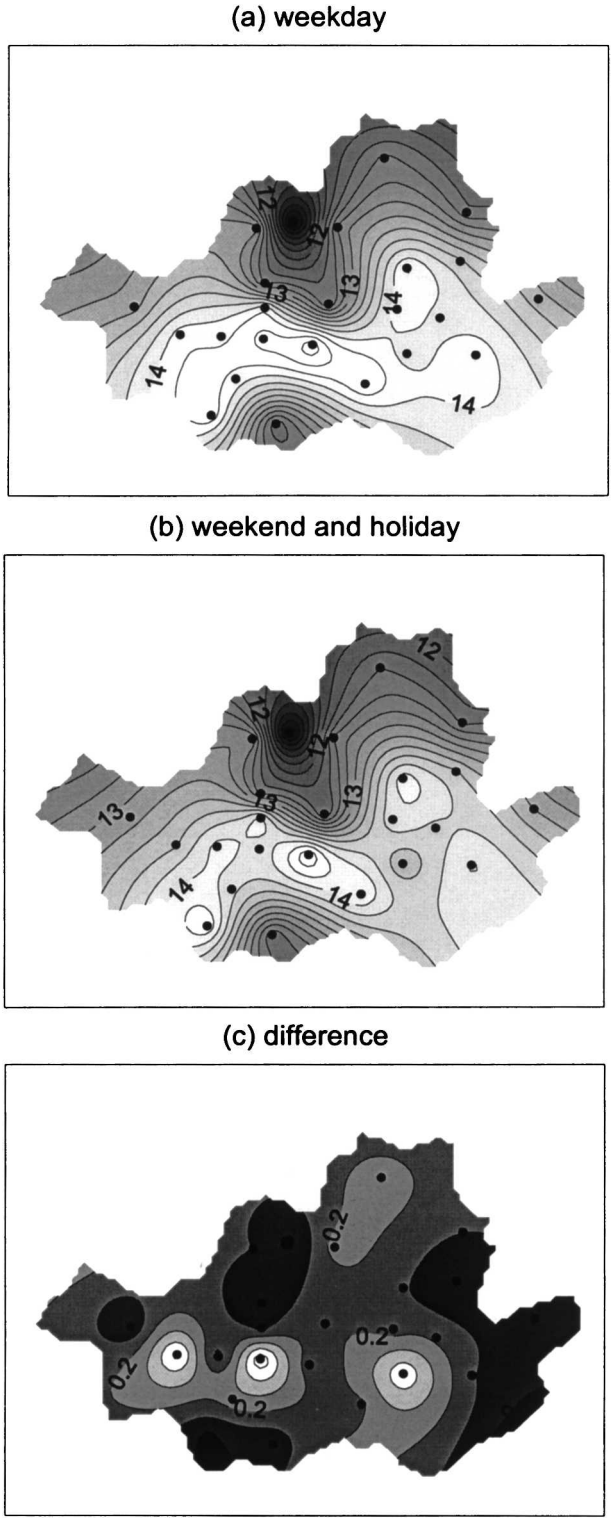

FIG. 14. Distribution of air temperature averaged for the 1-yr period Mar 2001–Feb 2002: (a) weekday temperature distribution, (b) weekend temperature distribution, and (c) weekday minus weekend temperature distribution. The contour interval is (a), (b) 0.2° and (c) 0.1°C, with lighter shading being larger values.

island was occasionally observed in the afternoon, but with its intensity being very weak. An empirical orthogonal function analysis enabled us to find the dominant modes of variability in the Seoul urban heat island. It was detected that the Seoul urban heat island is stronger on weekdays than weekends.

Several points deserve to be mentioned to promote further research on urban heat islands using AWS data. First, it would be interesting to stratify the near-surface temperature data according to typical synoptic weather conditions and investigate the spatial and temporal structure of the Seoul urban heat island under individual synoptic categories. This kind of research will contribute to our understanding of weather-regime influences on the Seoul urban heat island and will help to develop a more reliable statistical model for predicting the urban heat island intensity.

Second, an examination of the interannual variability of the Seoul urban heat island would be an interesting research topic when the accumulated AWS data of many years become available. For example, the structure of the urban heat island during an anomalously cold winter could be different, to some extent, from that during an anomalously warm winter. Global-scale phenomena (e.g., El Niño) can affect regional-scale circulations/weather, which, in turn, can affect the urban heat island. The interannual variability of the urban heat island intensity in connection with global-scale phenomena deserves an in-depth investigation.

Third, it is well known that precipitation anomalies exist within and around cities, in particular, that precipitation tends to increase downwind of an urban heat island (Changnon 1981). Therefore, it would be very interesting to examine to what extent precipitation anomalies within and around Seoul are related to the structure of the urban heat island. AWS temperature and precipitation data with high spatial and temporal resolutions would allow us to answer this question partly. This kind of research is expected to provide additional observational evidence for the theoretical modeling study (Baik et al. 2001), suggesting that an urban heat island can dynamically induce an updraft cell on its downwind side and initiate moist convection under a favorable thermodynamic environment, hence, contributing to precipitation enhancement on the downwind side.

Acknowledgments. The authors thank two anonymous reviewers for providing valuable comments and suggestions on this paper. They also thank Prof. Myung-Hee Jo of Kyungil University for providing the land use classification map of the Seoul metropolitan area. The second author was supported by the Climate Environment System Research Center, sponsored by the SRC Program of the Korea Science and Engineering Foundation, and also by the Brain Korea 21 Program.

REFERENCES

Arnfield, A. J., 2003: Two decades of urban climate research: A review of turbulence, exchanges of energy and water, and the urban heat island. *Int. J. Climatol.,* **23,** 1–26.

Baik, J.-J., Y.-H. Kim, and H.-Y. Chun, 2001: Dry and moist convection forced by an urban heat island. *J. Appl. Meteor.,* **40,** 1462–1475.

Boo, K.-O., and S.-N. Oh, 2000: Characteristics of spatial and temporal distribution of air temperature in Seoul (in Korean). *J. Korean Meteor. Soc.,* **36,** 499–506.

Bottyan, Z., and J. Unger, 2003: A multiple linear statistical model for estimating the mean maximum urban heat island. *Theor. Appl. Climatol.,* **75,** 233–243.

Byun, D. W., 1987: A two-dimensional mesoscale numerical model of St. Louis urban mixed layer. Ph.D. dissertation, North Carolina State University, 216 pp.

Changnon, S. A., Ed., 1981: *METROMEX: A Review and Summary*. *Meteor. Monogr.,* No. 40, Amer. Meteor. Soc., 181 pp.

Cotton, W. R., and R. A. Pielke, 1995: *Human Impacts on Weather and Climate*. Cambridge University Press, 288 pp.

Deosthali, V., 2000: Impact of rapid urban growth on heat and moisture islands in Pune city, India. *Atmos. Environ.,* **34,** 2745–2754.

Draxler, R. R., 1986: Simulated and observed influence of the nocturnal urban heat island on the local wind field. *J. Climate Appl. Meteor.,* **25,** 1125–1133.

Gallo, K. P., and T. W. Owen, 1999: Satellite-based adjustment for the urban heat island temperature bias. *J. Appl. Meteor.,* **38,** 806–813.

Garstang, M., P. D. Tyson, and G. D. Emmitt, 1975: The structure of heat islands. *Rev. Geophys. Space Phys.,* **13,** 139–165.

Ichinose, T., K. Shimodozono, and K. Hanaki, 1999: Impact of anthropogenic heat on urban climate in Tokyo. *Atmos. Environ.,* **33,** 3897–3909.

Jauregui, E., 1997: Heat island development in Mexico City. *Atmos. Environ.,* **31,** 3821–3831.

——, L. Godinez, and F. Cruz, 1992: Aspects of heat-island development in Guadalajara, Mexico. *Atmos. Environ.,* **26B,** 391–396.

Kim, Y.-H., and J.-J. Baik, 2002: Maximum urban heat island intensity in Seoul. *J. Appl. Meteor.,* **41,** 651–659.

——, and ——, 2004: Daily maximum urban heat island intensity in large cities of Korea. *Theor. Appl. Climatol.,* **79,** 151–164.

Klysik, K., and K. Fortuniak, 1999: Temporal and spatial characteristics of the urban heat island of Lodz, Poland. *Atmos. Environ.,* **33,** 3885–3895.

Korea Meteorological Administration, 2001: *Climatological Normals of Korea* (in Korean). KMA, 632 pp. [Available from Korea Meteorological Administration, 460-18 Sindaebang-dong, Dongjak-gu, Seoul 156-720, Korea.]

Landsberg, H. E., 1981: *The Urban Climates*. Academic Press, 275 pp.

Lin, Y.-L., and R. B. Smith, 1986: Transient dynamics of airflow near a local heat source. *J. Atmos. Sci.,* **43,** 40–49.

Montavez, J. P., A. Rodriguez, and J. I. Jimenez, 2000: A study of the urban heat island of Granada. *Int. J. Climatol.,* **20,** 899–911.

Morris, C. J. G., I. Simmonds, and N. Plummer, 2001: Quantification of the influences of wind and cloud on the nocturnal urban heat island of a large city. *J. Appl. Meteor.,* **40,** 169–182.

Oke, T. R., 1973: City size and the urban heat island. *Atmos. Environ.,* **7,** 769–779.

——, 1982: The energetic basis of the urban heat island. *Quart. J. Roy. Meteor. Soc.,* **108,** 1–24.
——, 1987: *Boundary Layer Climates*. 2d ed. Routledge, 435 pp.
Olfe, D. B., and R. L. Lee, 1971: Linearized calculations of urban heat island convection effects. *J. Atmos. Sci.,* **28,** 1374–1388.
Park, H.-S., 1986: Features of the heat island in Seoul and its surrounding cities. *Atmos. Environ.,* **20,** 1859–1866.
Peixoto, J. P., and A. H. Oort, 1992: *Physics of Climate*. American Institute of Physics, 520 pp.
Shepherd, J. M., H. Pierce, and A. J. Negri, 2002: Rainfall modification by major urban areas: Observations from spaceborne rain radar on the TRMM satellite. *J. Appl. Meteor.,* **41,** 689–701.
Wilks, D. S., 1995: *Statistical Methods in the Atmospheric Sciences*. International Geophysics Series, Vol. 59, Academic Press, 467 pp.
Yague, C., E. Zurita, and A. Martinez, 1991: Statistical analysis of the Madrid urban heat island. *Atmos. Environ.,* **25B,** 327–332.